Oligosaccharide Mimics Containing Galactose and Fucose Specifically Label Tumour Cell Surfaces and Inhibit Cell Adhesion to Fibronectin

Evelyn Y.-L. Kim,[a] Claas Gronewold,[a] Amitava Chatterjee,[b] Claus-Wilhelm von der Lieth,[c] Christian Kliem,[a] Birgit Schmauser,[a, d] Manfred Wiessler,*[a] and Eva Frei*[a]

With the aim of establishing a versatile and easy synthesis of branched saccharides for biological applications, we used molecular-dynamics simulations to model Lewis^y to two classes of di- or triantennary saccharide mimetics. One set of mimetics was based on 1,3,5-tris(hydroxymethyl)cyclohexane (TMC) as the core, the other on furan, and both were derivatised with galactose and/or fucose. The TMC-based saccharides were biotinylated, while the furan disaccharides were treated with maleimide-activated biotin in a Diels–Alder fashion to yield oxazatricyclodecanes (OTDs). These were then assayed as cell-surface labels in human colon (SW480 and CaCo-2), liver (PLC), Glia (U333 CG 343) and ovary (SKOV-3) tumour cell lines. Discrete staining patterns were observed in all cells, usually at one or two poles of the cells, particularly with the asymmetric 3-β-L-fucopyranosyloxymethyl-4-β-D-galactopyranosyloxymethyl-OTD. Normal SV40-transformed fibroblasts (SV80) showed no staining. Adhesion of the highly metastatic mouse melanoma line B16F10 to fibronectin was inhibited by 80% by the TMC-digalactoside and by 30% by 3,4-bis-(β-D-galactopyranosyloxymethyl)furan. None of the saccharide mimetics inhibited the adhesion of the less metastatic B16F1 line. Migration of B16F10 cells through Matrigel™ was greatly inhibited by the TMC-digalactoside and weakly inhibited by the TMC-trigalactoside. The saccharide mimetics that had shown the best structural agreements with the terminal saccharides of Lewis^y in the molecular dynamics simulation were also the most biologically potent compounds; this underlines the predictive nature of molecular dynamics simulations. The use of the non-saccharide cores enabled us to adapt spacer lengths and terminal saccharides to optimise the structures to bind more avidly to cell-surface lectins.

Introduction

Cell surfaces are highly glycosylated, either in the form of glycoproteins or glycolipids,[1] and the structural diversity of saccharides, particularly the different possible linkages in oligosaccharide chains, leads to a diversity far exceeding that of proteins or nucleic acids.[2] The information encoded by oligosaccharides on glycolipids or glycoproteins plays an essential role in protein folding, protein stability and cell–cell recognition. Lectins—proteins that specifically bind and recognise terminal saccharides in complex structures, first identified in plants and more recently in mammals—are partners capable of reading and recognising this glycocode. Binding of saccharides to lectins occurs in shallow binding sites with low affinity, unlike protein interactions with saccharides in enzymatic reactions, in which sugar binding has high affinity and occurs in deep clefts in the proteins. The affinity of saccharide ligands for lectins increases dramatically if the ligands are clustered and the distances between the terminal saccharides are optimal.[3,4] This was shown very systematically for the hepatic asialoglycoprotein receptor by Lee and Lee.[3] The asialoglycoprotein receptor is a heterotrimer in which each subunit has one CRD. The K_d values ranged from 0.5 mM for the monoantennary galactose ligand to 100 nM for the trivalent galactose cluster. For other sugar–lectin interactions, the structural requirements for potent inhibitors have also been analysed in terms of angles and distances of the ligand saccharides in glycoclusters, and are summarised in a review.[5] The distances between the binding saccharides are in the nanometer range. Cooperativity can also occur, however, if a second saccharide binds to a second CRD on the same subunit of a lectin; here distances would be expected to

[a] *Dr. E. Y.-L. Kim,[+] C. Gronewold,[+] Dr. C. Kliem, Dr. B. Schmauser, Dr. M. Wiessler, Dr. E. Frei*
Molecular Toxicology, Deutsches Krebsforschungszentrum
Im Neuenheimer Feld 280, 69120 Heidelberg (Germany)
Fax (+49) 6221-423-375
E-mail: m.wiessler@dkfz.de
e.frei@dkfz.de

[b] *Dr. A. Chatterjee*
Chittaranjan National Cancer Institute
S.P. Mukherjee Road 37, 700026 Kolkata (India)

[c] *Dr. C.-W. von der Lieth*
Central Spectroscopy, Deutsches Krebsforschungszentrum
Im Neuenheimer Feld 280, 69120 Heidelberg (Germany)

[d] *Dr. B. Schmauser*
Current address:
Bundesinstitut für Arzneimittel und Medizinprodukte (BfArM)
Abt. Pharmazeutische Qualität
Kurt-Georg-Kiesinger-Allee 3, 53175 Bonn (Germany)

[+] *These authors contributed equally to this work.*

  DOI: 10.1002/cbic.200400092

be shorter.[4] Galectins with just one or two CRDs can also cluster in response to multivalent saccharides, and as a consequence the otherwise weak binding is more avid.[6] Endogenous lectins are soluble or membrane-bound, and the role of lectin–saccharide interactions in tumour growth and progression is being intensively investigated. Cell–cell and cell–ECM adhesions are mediated not only by integrin–ligand interactions but also by lectin–oligosaccharide binding or saccharide–saccharide interactions. Such interactions of lectins with their oligosaccharide ligands can be perturbed by soluble saccharides, as demonstrated by Oguchi et al.,[7] who inhibited B16 melanoma metastasis to the lung by administration of methyl-α-D-lactose or lacto-*N*-tetrose.

Multiantennary saccharide structures would serve as good diagnostic tools or as inhibitors of cell migration and/or adhesion, were the synthesis of natural oligosaccharides not complicated and expensive. Saccharide mimetics that mimic the geometry of natural multiantennary oligosaccharides, however, should facilitate such applications.[2] Mimetics with easily accessible cores would also be ideal structures on which to optimise spacer lengths and terminal saccharides, to find the best fit to their "receptor".

We therefore modelled the terminal tetrasaccharide of Lewis^y, which is expressed in gastrointestinal, breast and lung carcinomas (summarised in ref. [8]), to two classes of di- or triantennary saccharide mimics. One mimetic is based on 1,3,5-tris(hydroxymethyl)cyclohexane (TMC) as core, its dimensions closely mimicking a pyranose, whilst the other mimics were products of Diels–Alder reactions between glycosylated furans and dienophile linkers (Scheme 1), with furan mimicking furanose. Molecular-dynamics (MD) simulations (with explicit water molecules) were performed to explore the conformational spaces of the new molecules and to derive geometric characteristics to enable easy comparison with the molecular shape of Lewis^y. We then proceeded to obtain information on the biological activity of the synthesised saccharide mimics in three assays. To detect binding of the mimics to cell surfaces, the TMC core was derivatised with two galactose moieties and biotin, while the diglycosylated furan was linked with biotin-maleimide in a Diels–Alder fashion (Scheme 2). The perturbation of the adhesion of B16F1 or B16F10 cells to fibronectin by the synthetic di- or trisaccharides was investigated, as was their influence on cell migration through Matrigel.

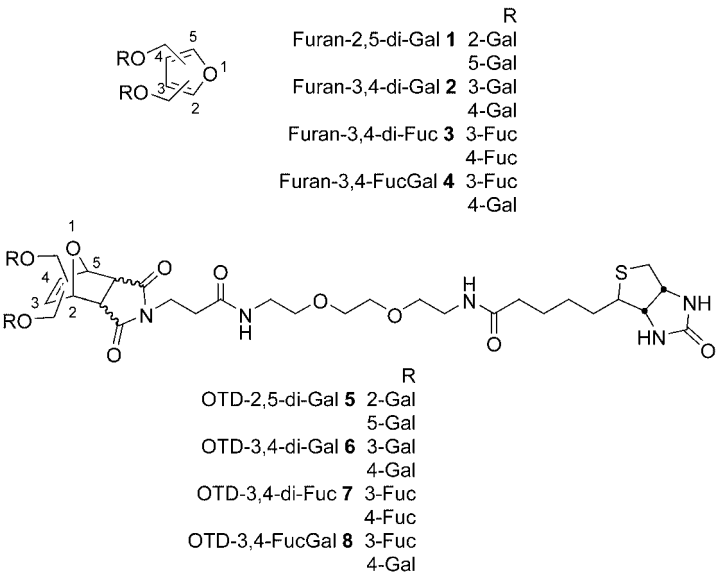

Scheme 1. *Structures of and abbreviations for the synthesised furan-derived saccharide mimetics used in the molecular dynamic simulations and for the biological assays.*

Results

Molecular dynamics simulations of the synthetic oligosaccharide mimics and Lewis^y

By analysing some meaningful structural features derived from MD simulations, we compared the TMC-galactosides (structures in Scheme 3) and the OTD-glycoside mimetics with the same structural characteristics of the tumour antigen Lewis^y.

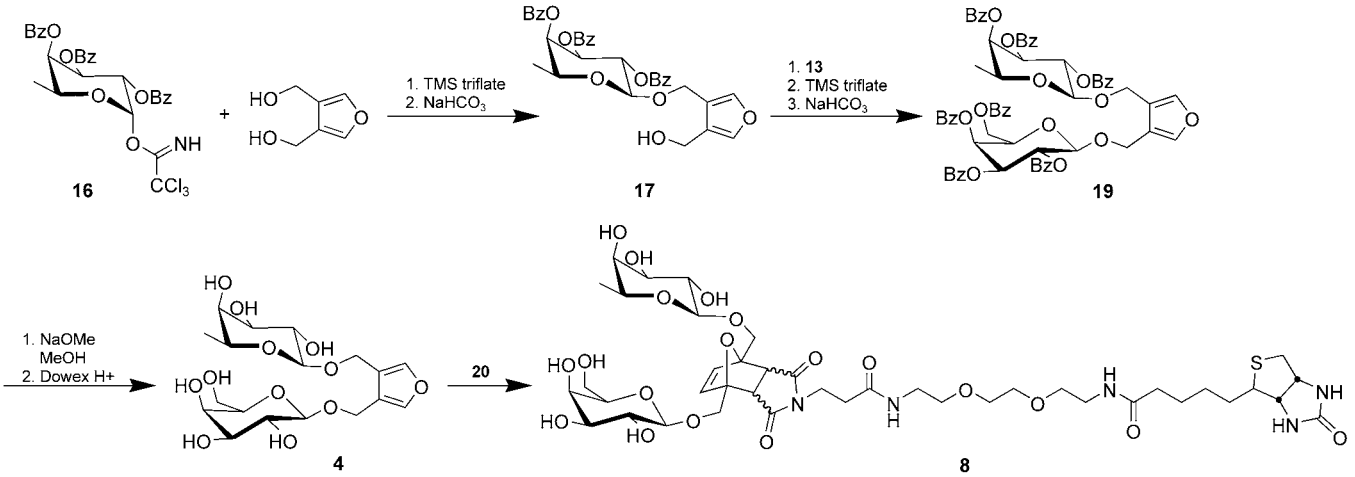

Scheme 2. *Synthesis of the furan-3,4-FucGal **4** as an example for the furan-based saccharide mimetics, together with the Diels–Alder reaction to provide the biotinylated OTD-3,4-FucGal **8**.*

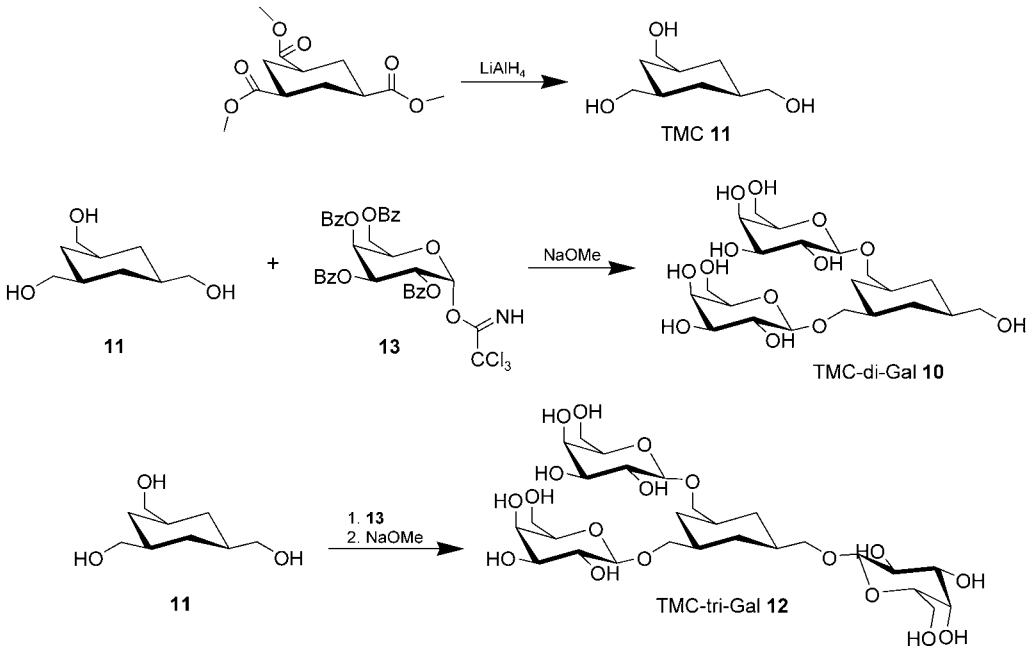

Scheme 3. *Synthesis of* cis,cis-*1,3-bis-(β-D-galactopyranosyloxymethyl)-5-(hydroxymethyl)cyclohexane (TMC-di-Gal; **10**) and* cis,cis-*1,3,5-tris-(β-D-galactopyranosyloxymethyl)cyclohexane (TMC-tri-Gal; **12**).*

For the oligosaccharide mimetics, the distances and angles formed by the centres of the core region and of each terminal sugar or of the three sugars were chosen as characteristic features. These values were compared with those derived for Lewis^y, with the two fucose and GlcNAc or Gal defined as relevant structures (Figure 1A). Simple three-point pharmacophore models based on the means and standard deviations of these characteristic features were derived and compared to the three-point models Gal-Fuc1-Fuc2 of Lewis^y (Figure 1B) or GlcNAc-Fuc1-Fuc2 (Figure 1C), because either Gal or GlcNAc could be involved in Lewis^y binding to a lectin.

The best alignment of the natural oligosaccharide was with the synthetic OTD-3,4-FucGal **8** when the OTD core was superimposed on GlcNAc of Lewis^y. Here, however, the Gal of the OTD mimic is superimposed on Fuc1 of Lewis^y (Figure 1C). If the Gal-Fuc1-Fuc2 triangle is compared with OTD-3,4-FucGal **8** (Figure 1B), the correct sugars are superimposed (Gal on Gal and Fuc on Fuc) and the fit is still good, because the standard deviations overlap. The 2,5-di-Gal derivative of OTD **5** does not align well with any Lewis^y pharmacophore model, because of its extended configuration. Replacement of Fuc by Gal in the OTD **8** does not result in a better fit, but the geometry is similar to that of TMC-di-Gal **10**. TMC-tri-Gal **12** showed very poor agreement with Lewis^y when the angles and distances of the centres of all three Gal units were matched to the terminal carbohydrates of Lewis^y.

No significant differences in geometry were observed when the furan was chosen as third centre instead of OTD. The orientation of the saccharides on the tricyclo ring system is therefore nearly identical to that in the original furan precursor in the Diels–Alder reaction.

Interactions of the biotinylated oligosaccharide mimics with the cell surface

When cells incubated with the biotinylated unsymmetrical diantennary OTD-3,4-FucGal **8** were treated with avidin-FITC, we observed discrete staining patterns with high fluorescent intensities on the cell surfaces of the two colon carcinoma cell lines SW480 (Figure 2C) and CaCo-2 (not shown), of the liver carcinoma PLC (Figure 2J) and of the ovarian carcinoma SKOV-3 (Figure 2I). The staining was either at one or at both poles on the cells, as can clearly be seen in Figure 2C for SW480 cells. The homologue OTD-3,4-mimics containing either two galactose or two fucose molecules showed altogether lower and diffuse fluorescence intensities (e.g., Figure 2B) except on the glia cells U-333, which were intensely labelled on treatment with the digalactoside (Figure 2L). Another exception was observed when SW480 cells were stained with OTD-3,4-di-Fuc **7**, which resulted in a discrete dipole staining pattern of the cells (Figure 2A). OTD-2,5-di-Gal **5**, however, showed a lower and diffuse staining pattern on these cell lines (data not shown). SKOV-3, when incubated with the biotinylated diantennary digalactoside of the TMC-series **9**, with a stereochemical orientation similar to that of the OTD-derived disaccharide mimetic, showed high fluorescence intensities both on the extracellular matrix and on the cells, where staining seemed to colocalise with focal adhesion points (Figure 2G). To show that the fluorescence staining is indeed localised on the cell membrane, SW480 cells were permeablised with Triton X-100 prior to the staining procedure. The oligosaccharide mimics then penetrated the cell and stained the nuclei intensely and the cytoskeleton weakly (Figure 2D). MCF-7 cells incubated with any

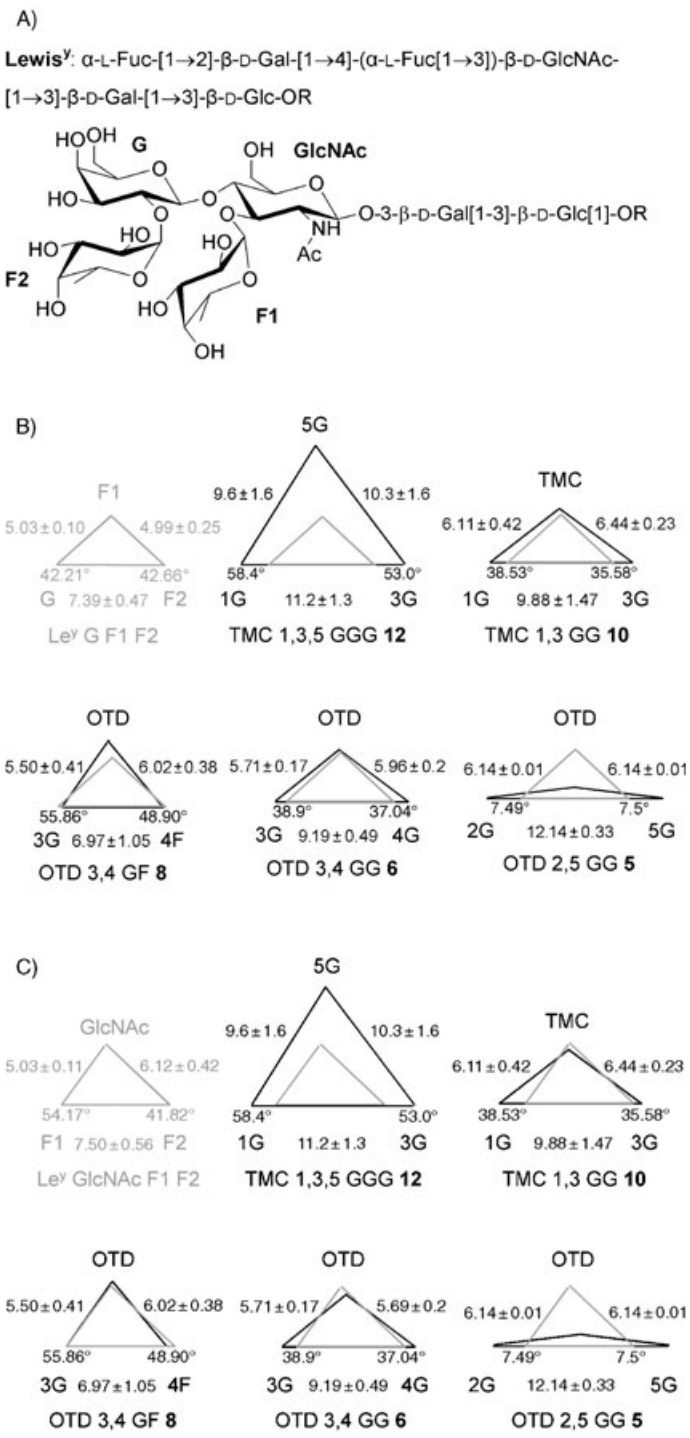

Figure 1. *Comparison of the defined characteristic geometric features of Lewis^y (A) with those of the synthetic carbohydrate mimetics. The statistical values of 1000 structures taken from the MD simulations are evaluated. B) Comparison of the centres of Gal, Fuc1 and Fuc2 in Lewis^y with those in the synthetic mimetics. C) Comparison of the centres of GlcNAc, Fuc1 and Fuc2 in Lewis^y with those in the synthetic mimetics (OTD: oxazatricyclodecane, G: galactose, F: fucose, TMC: 1,3,5-tris(hydroxymethyl)cyclohexane).*

of the OTD-3,4-disaccharides showed only weak and diffuse staining (data not shown). Only diffuse staining of some cells and spots on the ECM were also observed on normal human fibroblasts SV80 incubated with OTD-3,4-di-Gal **6** or OTD-2,5-di-Gal **5**, OTD-3,4-di-Fuc **7** or TMC-di-Gal **10** (Figure 2M, shown for OTD-3,4-di-Gal **6**). Cells incubated only with avidin-FITC were either dark or showed a very slight diffuse staining (not shown).

Adhesion assays with B16F1 and B16F10 cells on fibronectin

Another aspect of the biological effects of endogenous lectins is associated with their involvement in cell–cell or cell–extracellular matrix interactions and cell migration. Experiments were performed to determine whether our synthetic oligosaccharide mimics influenced the adhesion of cells to one ECM protein specifically and in a structure-related manner. The strengths of adhesion to fibronectin of B16F1 cells, which have low metastatic capacity in vivo, and of B16F10 cells, which are highly metastatic to the lung in syngeneic mice, were compared. The optimal amount of fibronectin per well was first determined to be 0.5 μg. Cells from both lines adhered very efficiently to fibronectin: 70% of the 50000 cells seeded per well were adhering after 1 h. No difference between the two lines was seen. Cells from both lines were then treated with different concentrations of TMC-di-Gal **10**, TMC-tri-Gal **12**, or with the control substances methyl β-D-galactopyranoside and the TMC core **11**. None of the compounds inhibited the adhesion of B16F1 cells to fibronectin (not shown). At 10 mM, however, the TMC-di-Gal **10** effectively inhibited the adhesion of B16F10 cells and at 40 mM cell adhesion was inhibited by 80%, while TMC-tri-Gal **12** and TMC **11** alone showed only 20% inhibition. Methyl β-D-galactopyranoside slightly promoted the adhesion of these cells to fibronectin at all concentrations tested (Figure 3A).

The two isomeric furan-digalactosides **1** and **2** also had different effects on the two cell lines. B16F1 adhesion was again not significantly affected by either galactoside, while B16F10 adhesion was inhibited by 40% by both furan mimetics at 20 and 40 mM. The stereochemical orientation of the two galactose moieties did not seem to influence the inhibitory potency, except at 10 mM, at which the 3,4-di-Gal isomer **2** slightly enhanced cell adhesion (Figure 3B). The unsymmetrical furan-3,4-FucGal **4** had no effect on B16F10 cells' adhesion to fibronectin.

None of the saccharide mimetics, nor TMC **11** nor methyl β-D-galactopyranoside was cytotoxic at the concentrations and incubation times used in our experiments, as determined by trypan blue exclusion. The osmolarity (Osmomat 030, Gonotec osmometer) of the medium was unchanged either by 50 mM TMC-tri-Gal **12** or by methyl β-D-galactopyranoside.

The inhibitory effects of the synthetic branched saccharide mimetics on cell adhesion to the ECM protein fibronectin are not unspecific effects of high saccharide concentrations, since methyl β-D-galactopyranoside either showed enhanced adhesion or had no effect.

Migration of B16F10 cells through Matrigel™

Because TMC-di-Gal **10** was the best inhibitor of cell adhesion while TMC-tri-Gal **12** was a weaker inhibitor, the TMC deriva-

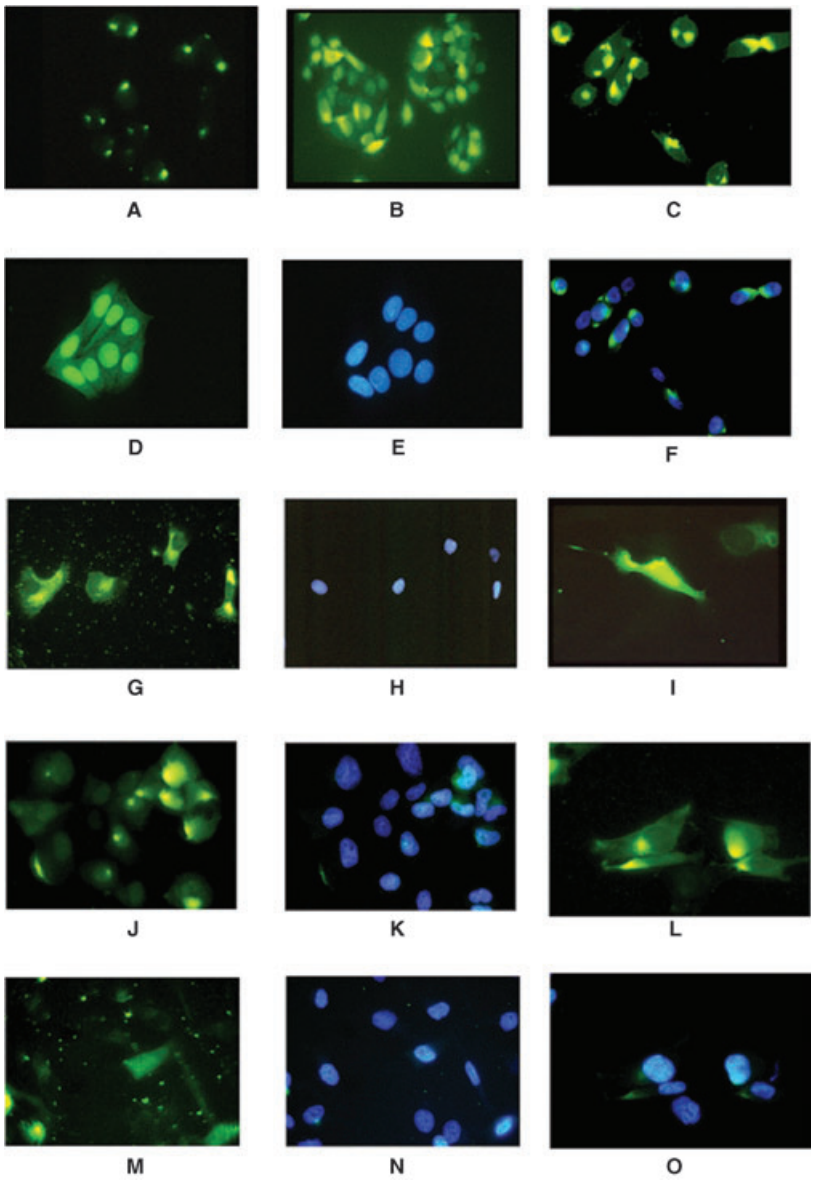

Figure 2. *Staining patterns obtained on cells after treatment with biotinylated OTD-3,4-di-Fuc* ***7*** *(A), OTD-3,4-di-Gal* ***6*** *(B, L, M), OTD-3,4-FucGal* ***8*** *(C, D, I, J,) or TMC-di-Gal* ***10*** *(G) and avidin-FITC. A–F are SW480 cells (colorectal adenocarcinoma), G–I are SKOV-3 (ovarian adenocarcinoma), J and K are PLC (liver carcinoma), L and O are glia (astrocytoma U333 CG 343) and M and N are SV80 (SV40 transformed fibroblasts). Pattern E shows the DAPI-stained nuclei of D, F those of C, H those of G, K those of J, N those of M, and O those of L. The cells in D and E were permeabilised with Triton-X100 prior to staining. All magnifications 100× except for L and O (200×).*

tives are a good model with which to investigate the influence of the number of galactose units in the mimetics on cell migration. The influence of the saccharide mimetics of the TMC series very closely paralleled the observations made in the adhesion assays. TMC-di-Gal **10** inhibited migration of B16F10 cells through this extracellular matrix preparation almost completely—Figure 4 shows the only cells to have migrated—while TMC-tri-Gal **12** only slightly inhibited migration. TMC **11** and methyl β-D-galactopyranoside slightly stimulated migration, more cells being visible on the lower side of the chamber than in the control incubations. The effect on B16F1 cells was similar, but more cells migrated in the presence of TMC-di-Gal **10** and cells tended to cluster (not shown). No toxicity of the compounds towards the cells was observed after 48 h, but TMC-di-Gal **10** and TMC-tri-Gal **12** inhibited cell growth. This growth inhibition is not relevant for the migration assay, since cells exposed to the saccharide mimetics are in serum-free medium and do not proliferate.

Discussion

The synthetic saccharide mimetics with either TMC or furan (derivatised to the Diels–Alder compound; OTD) units as core molecules bound to discrete areas on the surfaces of epithelial tumour cells. The staining pattern depended on the carbohydrate moieties, on their stereochemical orientation and on the tumour cell lines used.

The defined structural features, derived from MD simulations, could be successfully applied in order to compare the synthetic oligosaccharide mimics with Lewis^y, a branched oligosaccharide. In general, the results of the molecular modelling studies correlated very well with the findings of the biological experiments and also indicated some predictive power of this approach for the design of more potent inhibitors. The two compounds OTD-3,4-di-Gal **6** and the TMC-di-Gal **10**, which were biologically active, also showed the best structural correspondence with Lewis^y. OTD-2,5-di-Gal **5** stained cell surfaces only very weakly and in a diffuse way, while OTD-3,4-di-Gal **6** and particularly OTD-3,4-FucGal **8** showed discrete staining. TMC-di-Gal-biotin **9** also stained SKOV-3 cells specifically.

Normal human fibroblasts showed only very weak and diffuse staining, so these biotinylated saccharide mimetics seem to show specificity either for epithelial cells or maybe for tumour cells. The sites labelled by the biotinylated mimetics seem to be sites relevant for cell adhesion, since the furan-3,4-di-Gal **2** and particularly the TMC-di-Gal **10** effectively inhibited adhesion of the more metastatic murine melanoma cells B16F10 to fibronectin, while no effects were observable on the less metastatic B16F1 line. Both melanoma cell lines adhered

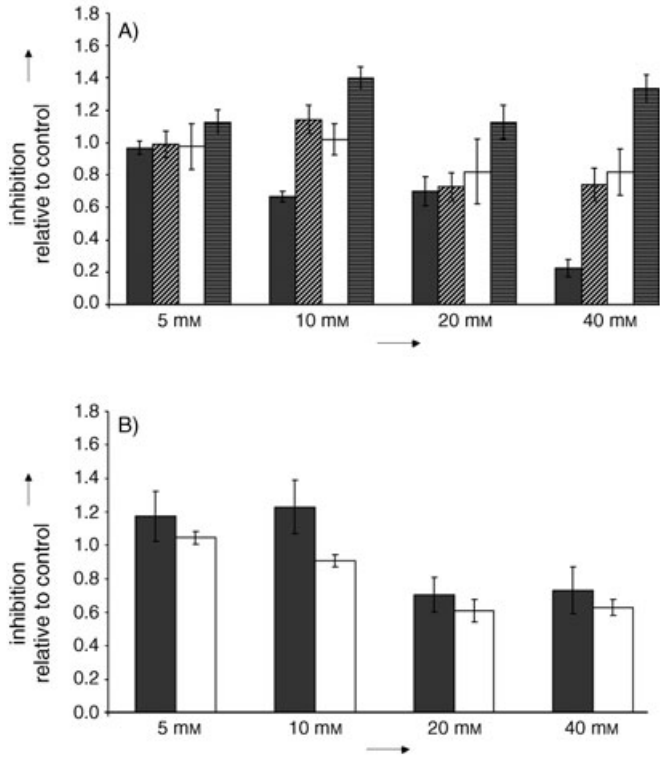

Figure 3. *Influence of adhesion of B16F10 cells to fibronectin of increasing concentrations of: A) TMC-di-Gal* ***10*** *(black bars), TMC-tri-Gal* ***12*** *(striped bars), TMC* ***11*** *(white bars) or methyl β-D-galactopyranoside (horizontally striped bars), and B) increasing concentrations of furan-3,4-di-Gal* ***2*** *(black bars) or furan-2,5-di-Gal* ***1*** *(white bars). Each well was coated with 0.5 μg fibronectin. Cells were labelled with [^{3}H]-thymidine, exposed to the test compounds for 1 h and seeded into the wells. After 1 h, nonadherent cells were washed away, radioactivity was counted, and the cell number was read from a calibration curve performed for each experiment. The values are means and standard deviations of four wells in relation to untreated cells (see Experimental Section for details).*

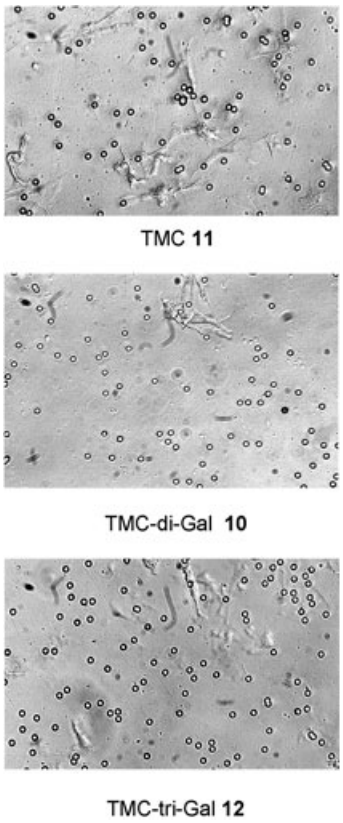

Figure 4. *Influence of 40 mM TMC derivatives on the migration of B16F10 cells through Matrigel™ after 48 h. The magnification was 200×. In the TMC-di-Gal* ***10*** *picture, these are the only cells that migrated. In the TMC-tri-Gal* ***12*** *insert, $^4/_5$ of the area was without cells; the area with cells is shown. In the control incubation without saccharides, fewer cells migrated than did in the presence of methyl β-D-galactopyranoside or TMC* ***11****; the picture represents a typical area. The round structures in the pictures are the pores of the membrane.*

equally strongly to fibronectin and both cell lines express $\alpha_5\beta_1$,[9,10] the fibronectin receptor.[11] TMC-di-Gal **10** also effectively inhibited migration of B16F10 and B16F1 cells through Matrigel, while TMC-tri-Gal **12** was less effective.

Chandrasekaran et al.[12] found cooperativity between a mannan-binding cellular lectin and β_1-integrin-mediated binding of B16F1 cells to laminin. Mannan binding to fixed adherent cells is localised in capping areas, while β_1 is located on the rims of cells in focal adhesion points. Our saccharide mimetics showed similar binding to poles or caps of cells, rather than to rims, except perhaps in the case of TMC-di-Gal **10** on SKOV-3 cells, which localised structures resembling focal adhesion plaques. The very intense and discrete staining of SW480 cells with OTD-3,4-FucGal **8** and OTD-3,4-di-Fuc **7** could be through binding to the fucose receptor described for these cells by Lerchen et al.[13]

Integrins consist of two subunits (α and β), associated noncovalently but tightly. Either subunit is coprecipitated with the antibody to the other subunit. The association of α_5 to β_1 seems to be controlled by the extent of N-glycosylation, since interference with this process dissociated the α_5 subunit from the β_1 subunit of the fibronectin receptor and at the same time decreased binding to fibronectin.[14] The same authors had previously observed a regulatory effect of G_{M3} (NeuAcα[2→3]Galβ[1→4]Glcβ[1→1]Cer), a glycosphingolipid, on $\alpha_5\beta_1$-mediated adhesion to fibronectin. Low G_{M3} concentrations enhanced adhesion, while high concentrations inhibited adhesion.[15] The saccharide mimetics used in our studies might similarly dissociate $\alpha_5\beta_1$ integrin, but they are highly water-soluble and are not integrated into the plasma membrane as sphingolipids are. Hakomori et al.[8] report that the expression level of G_{M3} in B16 cells correlates with their metastatic potential. The more metastatic B16F10 cells express more G_{M3} than B16F1. Raz et al., however, had earlier found no difference in G_{M3} levels between the two lines.[16]

A further possible means of carbohydrates perturbing integrin-mediated attachment to ECM proteins could be by binding to lectin domains on the integrins. The integrin subunit α_M in MAC-1, a leukocyte-specific integrin ($\alpha_M\beta_2$), has a lectin domain that, upon binding its carbohydrate ligand, triggers the neutrophile.[17] The α_5 or α_4 subunits might also have lectin-like properties enabling them to bind to the glyco structures in fibronectin, which would be perturbed by our soluble saccharide mimetics. These might also interfere with the association of

regulatory proteins with integrins. Such associations have been best examined on leukocytes.

The β_1 subunit and uPAR (urokinase-type plasmin activator receptor) can be co-immunoprecipitated from leukocyte membranes. This association is lectin/carbohydrate-mediated and can be perturbed by GlcNAc. uPAR is a ubiquitous regulatory protein, which also occurs on tumour cells and regulates integrin function by association–dissociation.[18]

Hangan-Steinmann et al.[10] observed that, in B16F1 cells expressing both $\alpha_5\beta_1$ and $\alpha_4\beta_1$ (both of which are fibronectin receptors), inhibition of binding to fibronectin with anti-α_5 plus anti-α_4 antibodies amounted to only 60%. The rest of the binding could therefore be mediated by oligosaccharide–lectin interactions.

Of the known lectins, galectins and selectins play important roles in cell adhesion processes.[19] Galectins 1 and 3 in particular seem to be important not only in tumour cell homotypic and heterotypic aggregation and clustering, which enhances formation of metastases, but also in adhesion to the ECM. Galectins recognise N-acetyl-lactosamines, and laminin and fibronectin contain poly-LacNAc structures and could therefore serve as galectin ligands.[20] Galectin 3, a soluble lectin, is overexpressed in various tumours, such as gastric, ovarian and breast. Galectin-1 binds laminin and fibronectin and may induce apoptosis, while galectin-3 inhibits anoikis, apoptosis induced by lack of adhesion.[1] Cell–cell aggregation is important for survival of metastasising cells, since B16F1 cells that aggregate form more pulmonary metastases.[21] This process seems to be saccharide-mediated, because citrus pectin containing branched oligosaccharides increases asialofetuin-induced cell aggregation and metastasis formation, while linear citrus pectin chains inhibit aggregation and metastases.[22]

Galectin 3 interacts with integrins in a concentration-dependent manner to enhance or attenuate integrin-mediated adhesion. Galactose can activate integrins to form clusters, which increases cellular adhesion to the ECM.[6] A similar mechanism could be the cause of the observed slight stimulation of B16F10 cell adhesion to fibronectin by methyl β-D-galactopyranoside.

Raz et al.[16] found no qualitative difference in protein composition, galactose or sialic acid content on the cell surfaces, or in membrane fluidity between B16F1 and B16F10 cells. Our finding of a difference in the inhibition of the binding of both lines to fibronectin by synthetic saccharides, despite similar initial binding, is one of the very few biochemical differences seen between these two lines. The tightness of binding to, as well as the amount of ECM around, a tumour cell determines its metastatic potential.[11] The relative ease with which B16F10 cells are prevented from binding to fibronectin after being "covered" with furan-3,4-di-Gal **2** or TMC-di-Gal **10** might reflect their ability to metastasise to the lung. B16F1 might express less of these relevant lectins and as a consequence not settle as easily in the lung.

Cell surface glycosylation can also change upon incubation with saccharides, as shown by Woynarowska et al.,[23] but after incubation times of 48–72 h. The effects we observed are therefore probably direct effects of the glycomimetics on cells.

These authors have shown that 3-deoxy-3-fluoro-*N*-acetylglucosamine and its 4-fluoro analogue can inhibit binding of ovarian cancer cells to galeptin, a Gal-binding ECM lectin isolated from human spleen. Their work shows that synthetic sugar mimetics can interfere with cell adhesion.[23]

The effective concentrations in our adhesion assays seem quite high, but are in the range cited in the literature.[24] Dissociation constants of oligosaccharide–protein complexes were found to be 10^{-3} to 10^{-4} M, and thus in the range of our effective saccharide concentration.[2] This could reflect suboptimal geometry of our synthetic compounds,[4] since multivalent ligands against, for example, cholera toxins with the proper terminal saccharide and spacer lengths, which fit the toxin binding sites, bind 10^7 times more avidly than monovalent saccharides.[25] The same happens with galectins—although they only contain either one or two CRDs, galectins are clustered by multivalent ligands.[26] Our synthetic strategy using mimetics as core molecules allows us to create libraries easily by changing spacer lengths and terminal saccharides to optimise the structures to bind more tightly to cell surface lectins.

Experimental Section

Molecular dynamics simulations: To explore the conformational space accessible to Lewis^y and the carbohydrate mimetics, MD simulations—including the aqueous surroundings—were performed. The applied modelling procedure was the same for all investigated structures, and performed according to a protocol recently described for analyses of glycoclusters and glycodendrimers.[5] One arbitrary 3D structure of each compound was placed in the centre of a 25×25×25 Å box, which was filled with water molecules. A double cut-off for nonbonded interactions of 10 and 12 Å was applied for a simulation period of 1 ns at a temperature of 400 K. One snapshot was stored every picosecond, and these 1000 structures were taken to perform the statistical analysis. The distances and angles between the centres of each pyranose ring on the one hand, and of the core regions of the glycomimetics on the other, were calculated as characteristic structural features to enable easy comparison of the investigated structures. For Lewis^y simulations the same internal co-ordinates were evaluated by using the centres of the two fucoses and the Gal or the GlcNAc residues as meaningful structural features. Evaluation of the statistics of the defined descriptors was accomplished with the aid of the Conformation Analysis Tool program developed by Frank.[27]

Chemical syntheses: ^{1}H NMR spectra were recorded on a Bruker AM250 spectrometer at 250 MHz; ^{13}C NMR chemical shifts were also obtained on a Bruker AM 250 (63 MHz) spectrometer. Mass spectroscopic data were performed on an Electrospray-Ionisation (ESI) Finnigan MAT TSQ7000 apparatus with an error of 0.5 mass units. All physicochemical measurements were performed in the Central Spectroscopy unit of the DKFZ.

Synthesis of the furan-derived carbohydrate mimetics (for structures see Scheme 1): 2,5-Bis-(β-D-galactopyranosyloxymethyl)furan (Furan-2,5-di-Gal; **1**), 3,4-bis-(β-D-galactopyranosyloxymethyl)furan (Furan-3,4-di-Gal; **2**), 3,4-bis-(β-L-fucopyranosyloxymethyl)furan (Furan-3,4-di-Fuc; **3**) and 3-β-L-fucopyranosyloxymethyl-4-β-D-galactopyranosyloxymethyl-furan (Furan-3,4-FucGal; **4**) were synthesised from 2,5-bis(hydroxymethyl)furan or 3,4-bis(hydroxymethyl)furan and the corresponding 2,3,4,5-tetra-*O*-benzoyl-β-D-galactopyranosyl trichloroacetimidate **13** and/or 2,3,4-tri-*O*-benzoyl-β-L-fucopyranosyl

trichloroacetimidate **16** under TMS triflate catalysis conditions. Deprotection of benzoylated diglycosylated bis-(hydroxymethyl)furans was with sodium methoxide. The detailed synthesis is described in ref. [28]. Diels–Alder reactions between the glycosylated bis-(hydroxymethyl)furans and EZ-Link™ PEO-maleimide activated biotin **20** (Pierce) yielded the oxazatricyclodecane derivatives (OTDs) **5**, **6**, **7** and **8** (see Scheme 2).

The numbering of the residues used in the OTD derivatives is the same as in the furan used in the Diels–Alder reaction to ease structural recognition of the compounds used in the biological assays.

Synthesis of the TMC-derived carbohydrate mimetics: *cis,cis*-1,3,5-Tris(hydroxymethyl)cyclohexane (TMC; **11**) was synthesised according to a published procedure.[29]

cis,cis-*1,3-Bis-(β-D-galactopyranosyloxymethyl)-5-(hydroxymethyl)cyclohexane (TMC-di-Gal; **10**; Scheme 3)*: TMS triflate (0.1 mL) was added at −40 °C to a solution of **11** (0.174 g, 1.0 mmol) and galactopyranosyl trichloroacetimidate **13** (1.85 g, 2.5 mmol) in CH_2Cl_2 (15 mL). The solution was then allowed to warm to 0 °C and allowed to react for 2 h. The reaction was quenched with $NaHCO_3$ (30 mL, 10% aqueous solution). The organic phase was separated, washed with H_2O (40 mL), dried over Na_2SO_4 and evaporated. The crude residue was crystallised from petrol ether/ethyl acetate (1:1) to give benzoylated **10**. The benzoylated intermediate in methanol (10 mL) was deprotected by treatment with excess sodium methoxide (13 mmol) in methanol (20 mL) with stirring at ambient temperature for 15 h. After neutralisation with Dowex WX8 H^+ the solvent was removed in vacuum. The crude residue was dissolved in water (30 mL) and washed thrice with diethyl ether (30 mL). The aqueous phase was evaporated, and the residue was purified by column chromatography on silica gel with acetonitrile/water (80:20) to yield **10** (0.2 mmol, 20%). ^{1}H NMR (250 MHz, $CDCl_3$): $\delta =$ 4.44 (d, ^3J(H-1′,H-2′) = 7.7 Hz, 2H; H-1′), 3.98 (dd, 2H; 2H-4′), 3.86 (dd, 2H; CH_{2a}), 3.85 (dd, ^3J(H-2′, H-3′) = 11.5 Hz, 2H; 2H-2), 3.8 (dd, 1H; H-3′), 3.72 (qd, ^3J(H-5′, H-6′a) = 3.3 Hz, ^3J(H-5′, H-6′b) = 7.7 Hz, 2H; 2H-5′), 3.7 (dd, ^2J(H-6′a, H-6′b) = 9.9 Hz, 2H; 2H-6′a), 3.6 (d, 2H; $2CH_{2b}$), 3.57 (dd, 2H; 2H-6′b), 3.52 (d, 2H; CH_2—OH), 1.56–2.0 (m, 6H; H-2a,b, H-4a,b, H-6a,b), 1.9–0.66 ppm (m, 3H; H-1, H-3, H-5); ^{13}C NMR (63 MHz, $CDCl_3$): $\delta =$ 107.65 (2C-1′), 80.24 ($2CH_2$), 79.63, 77.41, 75.41, 73.23 (2C-2′, 2C-3′, 2C-4′, 2C-5′), 71.76 (CH_2—OH), 65.48 (2C-6′), 42.94 (C-5), 40.96 (C-1, C-3), 36.37, 36.51, 36.44 ppm (C-2, C-4, C-6); MS-ESI: m/z (%): 521.2 [*M*+Na]$^+$ (100).

cis,cis-*1,3,5-Tris-(β-D-galactopyranosyloxymethyl)-cyclohexane* (TMC-tri-Gal; **12**): This compound was synthesised as described for **10**, with use of **11** (0.174 g, 1.0 mmol) and galactopyranosyl trichloroacetimidate **13** (2.59 g, 3.5 mmol). The benzoylated intermediate was deprotected as described above to yield **12** (0.55 mmol, 55%). ^{1}H NMR (250 MHz, $CDCl_3$): $\delta =$ 4.44 (d, ^3J(H-1′, H-2′) = 7.7 Hz, 3H, 3H-1′), 3.98 (dd, 3H; 3H-4′), 3.85 (dd, ^3J(H-2′, H-3′) = 11.5 Hz, 3H; 3H-2′), 3.8 (dd, 3H; 3H-3′), 3.72 (qd, ^3J(H-5′, H-6′a) = 3.3 Hz, ^3J(H-5′, H-6′b) = 7.6 Hz, 3H; 3H-5′), 3.7 (dd, ^2J(H-6′a, H-6′b) = 9.9 Hz, 3H; 3H-6′a), 3.6 (d, 6H; $3CH_2$), 3.57 (dd, 3H; 3H-6′b), 2.0–1.73 (m, 6H; H-2a,b, H-4a,b, H-6a,b), 0.8–0.62 ppm (m, 3H; H-1, H-3, H-5); ^{13}C NMR (63 MHz, $CDCl_3$): $\delta =$ 105.95 (3C-1′), 78.52, 77.93, 75.71, 73.73, (3C-2′, 3C-3′, 3C-4′, 3C-5′), 71.54 ($3CH_2$), 63.8 (3C-6′), 39.21 (C-1, C-3, C-5), 34.93 ppm (C-2, C-4, C-6); MS-ESI: m/z (%): 683.0 [*M*+Na]$^+$(100).

To synthesise the biotinylated TMC-digalactoside (**9**), the following procedure was followed (Scheme 4): 6-Chlorohexan-1-ol (7.5 mL, 56 mmol), NaN_3 (5.9 g, 91 mmol) and DMF (110 mL) were mixed together and kept at 70 °C overnight. Water (200 mL) was added to the reaction mixture, and the product was extracted into ether (3× 100 mL). The combined organic layers were washed with water, dried over Na_2SO_4 and evaporated to give a yellow-orange liquid. This liquid was used directly for the tosylation step. The solution of 6-azidohexan-1-ol and triethylamine (8.36 mL, 60 mmol) in CH_2Cl_2 (20 mL) was cooled to 0 °C, and tosyl chloride (11.4 g, 60 mmol) was added in portions to this reaction mixture. The temperature was allowed to rise to room temperature over 3 h. The reaction mixture was washed with water (3×100 mL), dried over Na_2SO_4, evaporated and then purified by column chromatography (petroleum ether/ethyl acetate 5:1) to give *p*-toluenesulfonic acid 6-azidohexyl ester **21** (9.5 g, 32.0 mmol, 57%) as a pale yellow liquid (this procedure is according to a personal communication from Yi Liu, Department of Chemistry and Biochemistry, University of California, Los Angeles). ^{1}H NMR ($CDCl_3$, 250 MHz): $\delta =$ 7.77 (d, $J =$ 8.1 Hz, 2H; 2×Ar–H), 7.33 (d, $J =$ 8.1 Hz, 2H; 2×Ar–H), 4.01 (t, $J =$ 6.4 Hz, 2H; CH_2—O), 3.20 (t, $J =$ 6.7 Hz, 2H; CH_2—N_3), 2.43 (s, 3H; CH_3), 1.73–1.60 (m, 2H; O–C–CH_2), 1.60–1.47 (m, 2H; N_3–C–CH_2), 1.42–1.26 ppm (m, 4H; O–C–C–CH_2–CH_2–C–C–N_3); MS-ESI (MeOH/$CHCl_3$): 298.2 ([*M*+H]$^+$, 30%), 315.2 ([*M*+NH_4]$^+$, 39%), 320.2 ([*M*+Na]$^+$, 100%), 617.3 ([2×*M*+Na]$^+$, 84%).

NaH (614 mg, 25.5 mmol) was added to a solution of **11** (4.45 g, 25.5 mmol) in DMF (30 mL) and the mixture was stirred for 1 h at 70 °C. Compound **21** (7.6 g, 34.4 mmol) in DMF (5 mL) was added dropwise to this suspension. After 4 h at 70 °C the solvent was removed under vacuum. The crude residue was dissolved in CH_2Cl_2 and washed with water (5×30 mL). The organic phase was dried over Na_2SO_4 and evaporated. The residue was purified by column chromatography on silica gel (petrol ether/ethyl acetate (2:1)) to yield *cis,cis*-1-(6-azidohex-1-yloxymethyl)-3,5-bis(hydroxymethyl)cyclohexane (**22**; 1.8 g, 6.0 mmol, 24%). ^{1}H NMR ($CDCl_3$, 250 MHz): $\delta =$ 3.49–3.30 (m, $J_{CH2\_O} =$ 5.8 Hz, $J_{CH2\_N3} =$ 6.5 Hz, 6H; CH_2–O, CH_2–N_3, OCH_2–cyclohexane), 3.25–3.17 (m, 4H; 2×HO–CH_2–cyclohexane), 1.93–1.73 (br m, 3H; 3×CH–cyclohexane), 1.62–1.46 (m, 7H; 3×CH–cyclohexane, O–C–CH_2, N_3–C–CH_2), 1.39–1.29 (m, 4H; C–C–CH_2–CH_2–C–C), 0.66–0.48 ppm (br m, 3H; 3×CH–cyclohexane); MS-ESI (MeOH/$CHCl_3$): 299.9 ([*M*+H]$^+$, 9%), 321.8 ([*M*+Na]$^+$, 77%), 621.1 ([2×*M*+H]$^+$, 100%).

cis,cis-*1-(6-Azidohex-1-yloxymethyl)-3,5-bis-(2′,3′,4′,6′-tetra-O-benzoyl-β-D-galactopyranosyloxymethyl)cyclohexane* (**23**): This compound was synthesised as described for **10** by use of **22** (897 mg, 3.0 mmol) and galactopyranosyl trichloroacetimidate **13** (5.5 g, 7.5 mmol). The crude product was purified by column chromatography on silica gel (petrol ether/ethyl acetate (2:1)) to yield **23** (1.44 g, 0.99 mmol, 33%). ^{1}H NMR ($CDCl_3$, 250 MHz): $\delta =$ 8.13–7.22 (m, 20H; 40×Ar–H), 5.98 (dd, $J_{3,4} =$ 3.4 Hz, $J_{4,5} =$ 0.7 Hz, 2H; 2×Gal-4-H), 5.74 (dd, $J_{1,2} =$ 7.8 Hz, $J_{2,3} =$ 10.1 Hz, 1H; Gal-2-H), 5.73 (dd, $J_{1,2} =$ 7.8 Hz, $J_{2,3} =$ 10.5 Hz, 1H; Gal-2-H), 5.59 (dd, 1H; Gal-3-H), 5.57 (dd, 1H; Gal-3-H), 4.69 (dd, $J_{5,6a} =$ 6.1 Hz, $J_{6a,6b} =$ 11.1 Hz, 1H; Gal-6a-H), 4.68 (dd, $J_{5,6a} =$ 6.1 Hz, 1H; Gal-6a-H), 4.58 (d, 1H; Gal-1-H), 4.56 (d, 1H; Gal-1-H), 4.40 (br dd, $J_{5,6b} =$ 6.3 Hz, 2H; 2×Gal-6-H), 4.26 (br t, 2H; 2×Gal-5-H), 3.69 and 3.65 (dd, $J =$ 10.0 Hz, $J =$ 4.9 Hz, 1H; CH–O-Gal), 3.25 (t, $J =$ 7.0 Hz, 2H; O–CH_2), 3.19 (t, $J =$ 6.8 Hz, 2H; N_3–CH_2), 3.07 and 3.01 (dd, $J =$ 9.7 Hz, $J =$ 6.3 Hz, 1H; CH–O-Gal), 2.84–2.73 (br m, 2H; CH_2–O–hexyl), 1.68–1.29 (m, 18H; 4× CH_2, 6 CH-cyclohexane), 0.50–0.25 ppm (m, 3H; 3×CH-cyclohexane); MS-ESI (MeOH/$CHCl_3$): 1471.7 ([*M*+NH_4]$^+$, 19%), 1478.6 ([*M*+Na]$^+$, 57%).

This benzoylated intermediate **23** (1.10 g, 0.76 mmol) was deprotected with NaOMe as described above to yield *cis,cis*-1-(6-azidohex-1-yloxymethyl)-3,5-bis-(β-D-galactopyranosyloxymethyl)cyclohexane (**24**) (250 mg, 0.40 mmol, 53%). ^{1}H NMR ([D_6]DMSO, 250 MHz): $\delta =$ 4.67 (d, $J =$ 4.1 Hz, 2H; 2×OH), 4.55 (d, $J =$ 3.7 Hz,

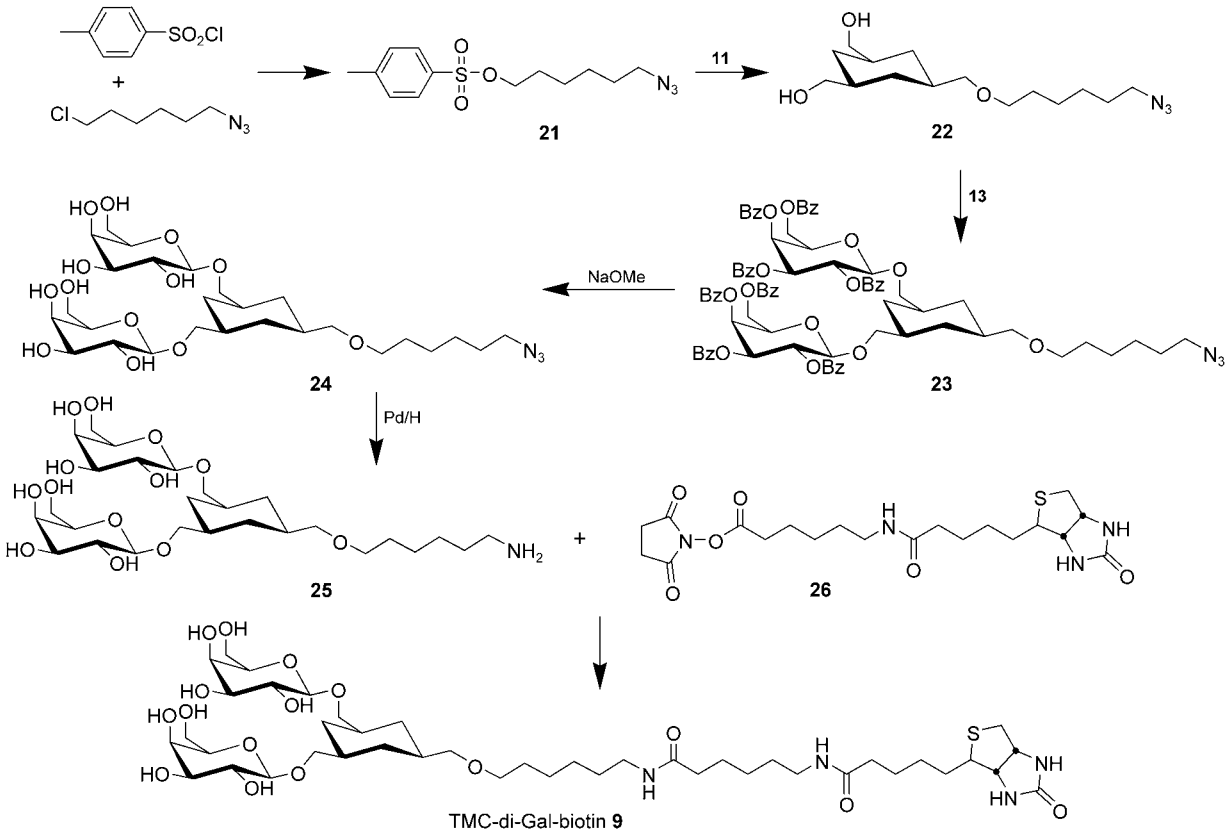

Scheme 4. *Synthesis of the biotinylated TMC-digalactoside* ***9****.*

2H; 2×OH), 4.46 (t, J=5.6 Hz, 2H; 2×Gal-6–OH), 4.24 (d, J=4.4 Hz, 2H; 2×OH), 4.04 (d, J=7.3 Hz, 2H; 2×Gal 1-H), 3.68–3.09 (m, 22H; 2×Gal-H-2, 2×Gal-H-3, 2×Gal-H-4, 2×Gal-H5, 4×Gal-H-6, 3×cyclohexane-CH_2–O, CH_2O, CH_2N_3), 2.22–1.72 (br m, 3H; 3×CH-cyclohexane), 1.69–1.41 (m, 7H; 3×CH-cyclohexane, O–C–CH_2, N_3–C–CH_2), 1.40–1.21 (m, 4H; C–C–CH_2–CH_2–C–C), 0.68–0.45 ppm (br m, 3H; 3×CH-cyclohexane); MS-ESI (MeOH): 624.4 ([M+H]$^+$, 2%), 646.4 ([M+Na]$^+$, 100%).

The solution of **24** (120 mg, 192 μmol) in MeOH (10 mL) was allowed to react in H_2 atmosphere in the presence of catalytic amounts of Pd/charcoal (10%) for 3 h. The catalyst was filtered through a short column packed with reversed-phase C-18 material and the solvent was removed in vacuum to yield pure *cis,cis*-1-(6-aminohex-1-yloxymethyl)-3,5-bis(β-D-galactopyranosyloxymethyl)-cyclohexane (**25**; 78.3 mg, 131 μmol, 68%). ^{1}H NMR ([D_6]DMSO, 250 MHz): δ=4.04 (d, J=6.8 Hz, 2H; 2×Gal-1-H), 3.65–3.11 (m, 22H; 2×Gal-H-2, 2×Gal-H-3, 2×Gal-H-4, 2×Gal-H5, 4×Gal-H-6, 3×cyclohexane-CH_2–O, CH_2O, CH_2N_3), 1.90–1.71 (br m, 3H; 3×CH-cyclohexane), 1.69–1.18 (m, 11H; 3×CH-cyclohexane, O–C–CH_2, N_3–C–CH_2, C–C–CH_2–CH_2–C–C), 0.69–0.47 ppm (br m, 3H; 3×CH-cyclohexane); MS-ESI (MeOH/H_2O): 598.4 ([M+H]$^+$, 100%), 620.3 ([M+Na]$^+$, 2%), 1196.0 ([2×M+H]$^+$, 4%).

Compound **25** was biotinylated by linking it to EZ-Link™ NHS-LC-Biotin (Pierce) by the manufacturers' instructions (http://www.piercenet.com) to yield TMC-di-Gal-biotin (**9**), except that residual NHS-activated biotin was treated with methylamine (10 μM), the solution was lyophilised, and the residue was taken up in PBS.

Cell lines and reagents: The following human cell lines were used for the experiments: SW480 (colorectal adenocarcinoma) and SKOV-3 (ovarian adenocarcinoma) were from the in-house tumour bank. CaCo-2 (colon adenocarcinoma ATCC HTB-37), SV80 (SV40-transformed fibroblasts), MCF-7 (mammary gland carcinoma ATCC HTB-22), Glioma (astrocytoma line U333 CG 343) and PLC (liver carcinoma ATCC CRL-8024) were kindly provided by L. Langbein (Cell Biology, DKFZ). The mouse melanoma cells B16F1 (ATCC CRL-6323) and B16F10 (ATCC CRL-6475) cells were purchased from American Type Culture Collection. Avidin-FITC was purchased from Sigma (Deisenhofen, Germany). Cells were maintained either in RPMI 1640 (SKOV-3 +15% FBS; SW480, U-333*)* or in DMEM (B16F1, B16F10, SV80, CaCo-2, PLC) supplemented with foetal bovine serum (10%). All cells were maintained at 37°C in a humidified atmosphere containing 5% CO_2. Mouse plasma fibronectin was from Invitrogen, Karlsruhe, Germany.

Fluorescence staining assay: Cells were grown on cover slips of 1 cm diameter. Before reaching confluence, cells were fixed for 10 min with formaldehyde in PBS (3%), washed with PBS (if cells were permeabilised they were treated with Triton X-100 (0.1%) in PBS for 10 min and washed), and unspecific binding sites were then blocked by treatment with milk powder (5%) in PBS for 1 h at RT or at 4°C overnight. Cells were then incubated with oligosaccharide mimic (40 μM) in BSA (0.1%) in PBS for 2 h at room temperature. Cover slips were washed with PBS/BSA. For fluorescence staining cells were incubated with avidin-FITC 1:100 in PBS/BSA for 1 h at room temperature. Nuclei were stained with DAPI (1 μg mL^{-1}). Cells were then washed with PBS, dried and embedded with Elvanol on glass slides. Microscopy was performed with a Leica microscope.

Adhesion assay: These assays were performed similarly to a published method.[24] Flexible 96-well plates were coated with fibro-

nectin (0.5 μg in 50 μL per well) at 4 °C overnight. Non specific binding sites were blocked with adhesion buffer (1 % BSA in PBS, 1 mM $CaCl_2$, 1 mM $MgCl_2$) for 1 h at 37 °C. To quantify adherent cells, B16F1 and B16F10 cells were labelled with [methyl-^{3}H]-thymidine (Amersham Life Science, 20 μCi per 10^6 cells) for 16 h at 37 °C and 5 % CO_2. The cells were then detached with EDTA (0.05 %) and washed three times with serum-free DMEM medium. The [methyl-^{3}H]-thymidine-labelled cells were resuspended in adhesion buffer (1 mL) containing the oligosaccharide mimics (5–40 mM): furan-2,5-di-Gal **1**, furan-3,4-di-Gal **2**, TMC-di-Gal **10**, TMC-tri-Gal **12** or the controls TMC **11**, methyl β-D-galactoside or medium only for 1 h at 37 °C with shaking. 5×10^4 cells were added to each fibronectin-coated well and allowed to settle for 1 h at 37 °C. Nonadherent cells were removed by washing three times with PBS. Each well was cut out, immersed in scintillation cocktail (Packard Ultima Gold XR) and counted (Packard TriCarb 2000 scintillation counter). For each experiment a calibration curve relating cell number to incorporated [methyl-^{3}H]-thymidine was performed. Four wells were run per experiment. The means and standard deviations in comparison with controls as calculated according to Bishop et al. are shown.[30]

Migration through Matrigel™: Hydrated Boydons invasion chambers for 24-well plates coated with Matrigel™, obtained from Becton–Dickinson, were immersed in medium (750 μL). B16F10 or B16F1 cells (4×10^5 mL^{-1}) in serum-free medium (500 μL) containing TMC **11**, TMC-di-Gal **10**, TMC-tri-Gal **12** or methyl β-D-galactoside (40 mM) were added to the top of the chamber and the system was incubated at 37 °C for two days. The cells that had not migrated were carefully brushed away with a cotton swab immersed in PBS. This procedure was repeated three times. The wells were inspected under a microscope and pictures were taken with a Leica camera.

Toxicity of the compounds over 48 h was determined with sulforhodamine-B.

Abbreviations

- CRD: carbohydrate recognition domain
- ECM: extracellular matrix
- TMC: 1,3,5-tris(hydroxymethyl)cyclohexane
- MD: molecular dynamics
- GlcNAc: 2-(*N*-acetyl)glucosamine
- OTD: oxazatricyclodecane
- DAPI: 4′,6-diamidino-2-phenylindole
- PBS: phosphate buffered saline
- BSA: bovine serum albumin
- FITC: fluorescein 5-isothiocyanate
- ESI-MS: electron spray ionisation mass spectrometry
- TMS triflate: trimethylsilyl trifluoromethanesulfonate
- uPAR: urokinase-type plasmin activator receptor.

Acknowledgements

We thank Dr. L. Langbein (Division of Cell Biology, Deutsches Krebsforschungszentrum) for providing the cell lines studied and for help with cell-staining experiments. Thanks are also due to the members of the Division of Spectroscopy for recording the NMR and ESI spectra of the synthesised compounds.

Keywords: biomimetic synthesis · carbohydrates · cell-surface lectins · extracellular matrix · molecular dynamics · molecular modeling

[1] E. Gorelik, U. Galili, A. Raz, *Cancer Metastasis Rev.* **2001**, *20*, 245–277.
[2] C. R. Bertozzi, L. L. Kiessling, *Science* **2001**, *291*, 2357–2364.
[3] Y. C. Lee, T. R. Lee, *Acc. Chem. Res.* **1995**, *28*, 321–327.
[4] W. I. Weis, K. Drickamer, *Annu. Rev. Biochem.* **1996**, *65*, 441–473.
[5] C-W. von der Lieth, M. Frank, T. K. Lindhorst, *Rev. Mol. Biotechnol.* **2002**, *90*, 311–337.
[6] R. C. Hughes, *Biochimie* **2001**, *83*, 667–676.
[7] H. Oguchi, T. Toyokuni, B. Dean, H. Ito, E. Otsuji, V. L. Jones, K. K. Sadozai, S. Hakomori, *Cancer Commun.* **1990**, *2*, 311–316.
[8] S. Hakomori. *Acta Anat.* **1998**, *161*, 79–90.
[9] S. Sengupta, S. Ray, N. Chattopadhyay, N. Biswas, A. Chatterjee, *J. Exp. Clin. Cancer Res.* **2000**, *19*, 81–87.
[10] D. Hangan-Steinmann, W. Ho, P. Shenoy, B. M. C. Chan, V. L. Morris, *Biochem. Cell Biol.* **1999**, *77*, 409–420.
[11] E. Ruoslathi, *Adv. Cancer Res.* **1999**,*76*, 1–20.
[12] S. Chandrasekaran, M. L. Tanzer, M. S. Ginger, *J. Biol. Chem.* **1994**, *269*, 3367–3373.
[13] H. G. Lerchen, J. Baumgarten, N. Piel, V. Kolb-Bachofen, *Angew. Chem.* **1999**, *111*, 3884–3888; *Angew. Chem. Int. Ed.* **1999**, *38*, 3680–3683.
[14] M. Zheng, H. Fang, S. Hakomori, *J. Biol. Chem.* **1994**, *269*, 12325–12331.
[15] M. Zheng, H. Fang, T. Tsuruoka, T. Tsuji, T. Sasaki, S. Hakomori, *J. Biol. Chem.* **1993**, *268*, 2217–2222.
[16] A. Raz, W. L. McLellan, I. R. Hart, C. D. Bucana, L. C. Hoyer, B. A. Sela, P. Dragsten, I. J. Fidler, *Cancer Res.* **1980**,*40*, 1645–1651.
[17] J. C. Porter, N. Hogg, *Trends Cell Biol.* **1998**, *8*, 390–396.
[18] H. R. Petty, R. G. Worth, R. F. Todd III, *Immunol. Res.* **2002**, *25*, 75–95.
[19] H. Kaltner, B. Stierstorfer, *Acta Anat.* **1998**, *161*: 162–179.
[20] K. Kasai, J. Hirabayashi, *J. Biochem.* **1996**, *119*, 1–8.
[21] A. Raz, C. Bucana, W. McLellan, I. J. Fidler, *Nature* **1980**, *284*, 363–364.
[22] H. Inohara, A. Raz, *Glycoconjugate J.* **1994**, *11*, 527–532.
[23] B. Woynarowska, D. M. Skricosky, A. Haag, M. Sharma, K. Matta, R. J. Bernacki, *J. Biol. Chem.* **1994**, *269*, 22797–22803.
[24] N. Kojima, M. Shiota, Y. Sadahira, K. Handa, S. Hakomori, *J. Biol. Chem.* **1992**, *267*, 17264–17270.
[25] P. I. Kitov, J. M. Sadowska, G. Mulvey G. D. Armstrong, H. Ling, N. S. Pannu, R. J. Read, D. R. Bundle, *Nature* **2000**, *403*, 669–672.
[26] H. Inohara, A. Raz, *Cancer Res.* **1995**, *55*, 3267–3271.
[27] M. Frank, Dissertation Universität Heidelberg (Germany) **2000** http://www.ub.uni-heidelberg.de/archiv/605.
[28] M. Wiessler, H. Hoffmann, B. Meister, S. Wolf, E. Mark, C. Tacheci, B. Schmauser, B. Sauerbrei, C. Kliem, unpublished results (http://www.dkfz-heidelberg.de/spec/publications/suppl_mat/diels_alder/)
[29] M. S. Newman, H. S. Lowrie, *J. Am. Chem. Soc.* **1954**, *76*, 4598–4600.
[30] Y. M. M. Bishop, S. E. Fienberg, P. W. Holland, *Discrete Multivariante Analysis: Theory and Practice*, MIT Press, Cambridge MA, **1975**.

Received: April 5, 2004
Revised: August 30, 2004
Published online: January 13, 2005

